10:55～11:40

セッションⅡ 【病因・病態Ⅱ】 座長：**佐々木秀直**（北海道大学神経内科）

4. 神経変性の謎に迫る：ミトコンドリアの損傷と排除

○田中（たなか） 啓二（けいじ）、松田 憲之
東京都臨床医学総合研究所

5. 神経突起様伸長及び増殖を制御するTRIM-EN1/2の機能解析

○矢口（やぐち） 裕章（ひろあき）[1),2)]、奥村 文彦[2)]、加納 崇裕[1),2)]、渡部 昌[2)]、
内ヶ島基政[3)]、渡邊 雅彦[3)]、畠山 鎮次[2)]、佐々木秀直[1)]
1) 北海道大学神経内科学
2) 北海道大学医化学
3) 北海道大学解剖発生学

6. ヒトiPS細胞の神経分化と疾患モデルiPS細胞

○岡野（おかの） 栄之（ひでゆき）[1),2)]、岡田 洋平[1),2)]
1) 慶應義塾大学生理学教室
2) 咸臨丸プロジェクト

11:40～12:25

セッションⅢ 【治療Ⅰ（血管新生因子・HGF）】

座長：**青木 正志**（東北大学神経内科）

7. 血管新生因子によるALSモデルラット神経保護の試み

○割田（わりた） 仁（ひとし）[1)]、水野 秀紀[1)]、鈴木 直輝[1)]、船越 洋[2)]、
中村 敏一[3)]、糸山 泰人[4)]、青木 正志[1)]
1) 東北大学神経内科，東北大学病院ALS治療開発センター
2) 大阪大学分子再生医学
3) 大阪大学先端科学イノベーションセンター再生創薬共同研究部門
4) 国立精神・神経医療研究センター病院

8. 運動神経細胞でHGFを発現するポリオウイルスベクターの開発

千葉　妃織[1)]、端川　　勉[2)]、五十嵐博子[1)]、○大岡（おおおか）　静衣（せいい）[1),3)]、
大谷　若菜[4)]、船越　　洋[4)]、中村　敏一[5)]、野本　明男[1),6)]

1) 東京大学微生物学講座
2) 理化学研究所研究基盤センター脳形態解析支援ユニット
3) 独立行政法人国立がん研究センター研究所がん幹細胞研究分野
4) 大阪大学分子再生医学
5) 大阪大学先端イノベーションセンター
6) 微生物化学研究所

9. ALSに対するHGFの至適供給法の検討―各蛋白質供給法と遺伝子治療法を比較して

○船越　　洋[1)]、角山　圭一[1),2)]、島田（大谷）若菜[3)]、
青木　正志[4)]、糸山　泰人[5)]、宮武　伸一[6)]、R.S. Coffin[7)]、
水上　浩明[8)]、小澤　敬也[8)]、中村　敏一[3)]

1) 大阪大学ウイルス学／分子再生医学
2) 姫路独協薬科大学
3) 大阪先端科学イノベーションセンター
4) 東北大学神経内科
5) 国立精神神経医療センター病院
6) 大阪医科大学脳外科
7) London大学
8) 自治医科大学

12:25～13:15　　＊＊＊＊＊＊ 昼食・班会議 ＊＊＊＊＊＊

13:15～14:00

セッションⅣ 【治療Ⅱ（低分子化合物・遺伝子治療）】

座長：**高橋　良輔**（京都大学神経内科）

10. キサンチン酸化還元酵素（XOR）阻害作用を有しかつプリンサルベージ回路の基質とならない化合物としてのALS治療薬

○加藤（かとう）　信介（しんすけ）[1)]、加藤　雅子[2)]、西野　武士[3)]

1) 鳥取大学脳神経病態医科学分野

2) 鳥取大学分子病理学分野

3) 米国カルフォルニア大学生化学分野

11. 転写を標的とした家族性筋萎縮性側索硬化症新規治療法の開発

○村上（むらかみ）　学（がく）[1)]、井上　治久[2)]、月田香代子[2)]、淺井　康行[3)]、天貝　裕地[4)]、饗庭　一博[4)]、下川　浩輝[5)]、上杉　志成[5)]、中辻　憲夫[6)]、高橋　良輔[1)]

1) 京都大学臨床神経学

2) 京都大学iPS細胞研究センター（CiRA）

3) (株) リプロセル

4) 幹細胞創薬研究所

5) 京都大学化学研究所生体機能化学研究系

6) 京都大学物質ー細胞統合システム拠点

12. 血管内投与型AAVベクターによる希突起膠細胞への遺伝子導入

○村松（むらまつ）　慎一（しんいち）[1)]、奈良　優子[1)]、宮内ひとみ[1)]、綾部　啓子[1)]、滝野　直美[1)]、中野　今治[1)]、島崎久仁子[2)]

1) 自治医科大学神経内科学

2) 自治医科大学神経脳生理

14:00～14:45

セッションV 【治療Ⅲ（免疫関連治療）】

座長：漆谷　真（滋賀医科大学分子神経科学研究センター）

13. ALSの免疫療法における野生型SOD1の応用性について

大野　美樹[1),2)]、竹内　成子[1)]、井戸　明美[1)]、高橋　良輔[2)]、
○漆谷（うるしたに）　真（まこと）[1)]

1) 滋賀医科大学分子神経科学研究センター

2) 京都大学神経内科

14. ALSモデルマウスにおける骨髄移植と顆粒球コロニー刺激因子投与の併用効果

阿部　康二、太田　康之、○森本（もりもと）　展年（のぶとし）、宮崎　一徳、
池田　佳生、松浦　徹

岡山大学脳神経内科学

15. B細胞刺激因子（BAFF）はALSモデル動物の神経変性を抑制する

○多田（ただ）　智（さとる）[1)]、安居　輝人[2)]、奥野　龍禎[1),3)]、中辻　裕司[1)]、
菊谷　仁[2)]、佐古田三郎[4)]

1) 大阪大学神経内科

2) 大阪大学微生物病研究所分子免疫制御分野

3) 大阪大学微生物病研究所感染病態分野

4) 国立病院機構刀根山病院

14:45～15:00　　休　憩

15:00～16:00

セッションVI 【TDP-43】　　座長：横田　隆徳（東京医科歯科大学神経内科）

16.　酸化ストレスによるTDP-43修飾の検討

○井口（いぐち）　洋平（ようへい）[1)]、勝野　雅央[1),2)]、高木伸之介[1)]、田中　章景[1)]、
祖父江　元[1)]
1) 名古屋大学神経内科
2) 名古屋大学・高等研究院

17.　TDP-43凝集体形成による神経細胞毒性の誘導

○山下万貴子（やましたまきこ）、野中　　隆、亀谷富由樹、辻　　浩史、
細川　雅人、秋山　治彦、長谷川成人
東京都精神医学総合研究所

18.　ALS運動ニューロンにおけるRNA編集異常とTDP-43病理

○山下（やました）　雄也（たけなり）、日出山拓人、寺本さやか、八賀　康祐、
郭　　伸
東京大学神経内科

19.　野生型TDP-43過剰発現によるALS動物モデルの作製

水澤　英洋、内田あずさ、笹栗　弘貴、田尻　美緒、
佐野　達彦、上野　智美、小林　正樹、大久保卓哉、
久保寺隆行、○横田（よこた）　隆徳（たかのり）
東京医科歯科大学脳神経病態学分野

VI. 研究者一覧

平成22年度厚生労働科学研究費補助金（難治性疾患克服研究事業）
「筋萎縮性側索硬化症の病態に基づく画期的治療法の開発」班（課題番号　H20-難治-一般-045）
研究者一覧

区　分	氏　名	所　属　等	職　名
研究代表者	祖父江　元	名古屋大学大学院医学系研究科 細胞情報医学専攻脳神経病態制御学講座 神経内科学分野	教授
研究分担者	岡野　栄之	慶応義塾大学医学部 生理学教室	教授
	郭　　伸	東京大学大学院医学系研究科 脳神経医学専攻臨床神経精神医学講座 神経内科学分野	准教授
	高橋　良輔	京都大学大学院医学研究科 脳病態生理学講座 臨床神経学分野	教授
	田中　啓二	東京都臨床医学総合研究所 先端医学センター （生体分子遺伝学）	所長代行
	中野　今治	自治医科大学 内科学講座 神経内科学部門	教授
	青木　正志	東北大学大学院医学系研究科 神経学講座 神経内科学分野	教授
	船越　　洋	大阪大学大学院医学系研究科 未来医療開発専攻組織再生医学講座 分子組織再生分野	准教授
	漆谷　　真	滋賀医科大学 分子神経科学研究センター 難病治療学分野	准教授
	長谷川　成人	東京都精神医学総合研究所 分子神経生物学研究チーム	副参事研究員
	山中　宏二	理化学研究所 脳科学総合研究センター	チームリーダー
研究協力者	阿部　康二	岡山大学大学院医歯薬学総合研究科 神経病態内科学講座 神経内科学分野	教授
	加藤　信介	鳥取大学医学部 脳病態医科学分野	准教授
	加藤　丈夫	山形大学医学部 器官病態統御学講座 生命情報内科学分野	教授
	佐々木　秀直	北海道大学大学院医学研究科 神経内科	教授
	佐古田　三郎	国立病院機構刀根山病院 神経内科	院長
	谷口　直之	大阪大学産業科学研究所 疾患糖鎖学（生化学工業）寄付研究部門	教授
	野本　明男	（財）微生物化学研究会微生物研究センター	理事長
	水澤　英洋	東京医科歯科大学大学院医歯学総合研究科 脳神経病態学講座 神経内科学分野	教授

Ⅶ. 研究成果の刊行物・別刷

Journal of Neuroscience Research 88:123–135 (2010)

Dorfin Ameliorates Phenotypes in a Transgenic Mouse Model of Amyotrophic Lateral Sclerosis

Jun Sone,[1] Jun-ichi Niwa,[1,2] Kaori Kawai,[1] Shinsuke Ishigaki,[1] Shin-ichi Yamada,[1] Hiroaki Adachi,[1] Masahisa Katsuno,[1] Fumiaki Tanaka,[1] Manabu Doyu,[1,2] and Gen Sobue[1]*

[1]Department of Neurology, Nagoya University Graduate School of Medicine, Nagoya, Japan
[2]Department of Neurology and Stroke Center, Aichi Medical University, Aichi, Japan

Amyotrophic lateral sclerosis (ALS) is a fatal neurodegenerative disease that is characterized by progressive motor neuron degeneration and leads to death within a few years of diagnosis. One of the pathogenic mechanisms of ALS is proposed to be a dysfunction in the protein quality-control machinery. Dorfin has been identified as a ubiquitin ligase (E3) that recognizes and ubiquitinates mutant SOD1 proteins, thereby accelerating their degradation and reducing their cellular toxicity. We examined the effects of human Dorfin overexpression in G93A mutant SOD1 transgenic mice, a mouse model of familial ALS. In addition to causing a decrease in the amount of mutant SOD1 protein in the spinal cord, Dorfin overexpression ameliorated neurological phenotypes and motor neuron degeneration. Our results indicate that Dorfin overexpression or the activation or induction of E3 may be a therapeutic avenue for mutant SOD1-associated ALS.

Key words: Dorfin; ALS; G93A mutant SOD1; ubiquitin ligase; neurodegeneration

Amyotrophic lateral sclerosis (ALS) is a progressive and fatal neurodegenerative disease characterized by progressive muscle atrophy, paralysis, and death within a few years of diagnosis (Rowland and Shneider, 2001). Several hypotheses for the pathogenesis of ALS have been proposed, including protein quality-control dysfunction, mitochondrial damage, oxidative stress, glutamate receptor abnormality, inflammation, neurotrophic factor deficiency, and activation of apoptosis (Julien, 2001; Boillee et al., 2006; Kabashi and Durham, 2006; Cassina et al., 2008). However, the pathogenic mechanism has not been clarified, and no effective therapy has been developed. Approximately 90% of ALS cases are sporadic (nonhereditary; SALS) and 10% are familial ALS (hereditary; FALS). About 20% of cases of FALS are due to mutations in Cu/Zn superoxide dismutase 1 (SOD1; Rosen et al., 1993; Hirano, 1996; Martin et al., 2007). Mutant SOD1 protein is thought to induce motor neuron degeneration by a gain of toxic function rather than a loss of dismutase function (Bruijn et al., 1998; Boillee et al., 2006; Martin et al., 2007).

Sporadic and familial ALS present inclusion bodies composed of aberrant protein aggregates in the cytoplasm of residual motor neurons (Shibata et al., 1996; Ross and Poirier, 2004; Strong et al., 2005). Inclusions containing mutant SOD1 are found in the motor neurons of mutant SOD1-related FALS patients and mutant SOD1 transgenic (Tg) mice (Gurney et al., 1994; Shibata et al., 1996; Watanabe et al., 2001). Aberrant proteins such as mutant SOD1 are ubiquitinated (Alves-Rodrigues et al., 1998; Ardley and Robinson, 2004) and are thought to be degraded by the ubiquitin-proteasome system (Niwa et al., 2002; Urushitani et al., 2002; Goldberg, 2003; Kabuta et al., 2006; Cheroni et al., 2009). However, when the production of aberrant proteins exceeds the cellular degradation capacity, these proteins often form aggregates before they are degraded (Sherman and Goldberg, 2001; Goldberg, 2003).

The ubiquitin-proteasome system mediates post-translational modification and degradation of proteins and is essential for many fundamental cellular functions, including cell cycling, DNA repair, cell signaling, gene transcription, and apoptosis (Ardley and Robinson, 2004; Kabashi and Durham, 2006). Protein ubiquitination is an ATP-dependent process during which ubiquitin is sequentially activated by ubiquitin-activating enzymes (E1), transferred to ubiquitin-conjugating enzymes (E2),

Contract grant sponsor: 21st Century Center of Excellence (COE) grant and global COE grant from the Ministry of Education, Culture, Sports, Science and Technology of Japan; Contract grant sponsor: Ministry of Health, Welfare and Labor of Japan; Contract grant sponsor: Core Research for Evolutional Science and Technology.

*Correspondence to: Gen Sobue, MD, Department of Neurology, Nagoya University Graduate School of Medicine, Nagoya 466-8550, Japan. E-mail: sobueg@med.nagoya-u.ac.jp

Received 22 January 2009; Revised 20 May 2009; Accepted 24 May 2009

Published online 16 July 2009 in Wiley InterScience (www.interscience.wiley.com). DOI: 10.1002/jnr.22175

and ligated to protein substrates by ubiquitin ligases (E3). Polyubiquitinated proteins are degraded by the 26S proteasome (Goldberg, 2003; Ciechanover, 2005). E3s are of particular importance insofar as they determine the targeting specificity of the ubiquitin-proteasome system (Ardley and Robinson, 2004).

Previously, we identified Dorfin as the product of a gene expressed in the anterior horn of the human spinal cord (Niwa et al., 2001). Dorfin contains a RING-finger/in-between-RING domain and functions as an E3. Dorfin is the first E3 reported to recognize mutant SOD1 proteins and to accelerate their degradation, thereby reducing their cellular toxicity in vitro (Niwa et al., 2002; Takeuchi et al., 2004). We have also shown that Dorfin is located in the inclusions found in spinal cord sections from SALS, FALS, and other neurodegenerative disease patients (Niwa et al., 2002; Hishikawa et al., 2003; Ito et al., 2003). These results suggest that Dorfin is involved in the protein quality-control system that addresses abnormal proteins related to neuronal degeneration. In particular, the results suggest that Dorfin acts in vivo as an E3, which reduces the level of mutant SOD1 aggregates and toxicity.

In this study, we demonstrate that transgenic overexpression of Dorfin ameliorated phenotypic expression in G93A mutant SOD1 transgenic mice and reduced the accumulation of mutant SOD1 in the spinal cord. These results suggest that Dorfin overexpression may be an effective treatment for mutant SOD1-related FALS.

MATERIALS AND METHODS

Generation and Maintenance of Tg Mice and Genotyping

Full-length human Dorfin cDNA (GenBank accession No. AB029316) tagged with the FLAG epitope was amplified by PCR and inserted into a pCMV-Tag2 vector (Stratagene, La Jolla, CA). FLAG-Dorfin was excised from the vector and inserted downstream of the chicken β-actin promoter in the pCAGGS vector (see Fig. 1A). We generated Dorfin Tg mice by microinjection of pCAGGS carrying FLAG-Dorfin into BDF1 fertilized eggs and obtained 20 founders. These founder mice were back-crossed to C57BL/6 mice. We screened mouse tail DNA by PCR for the presence of the Dorfin transgene using the primers 5-TTGATTTATATTTTGGC GATGC-3 and 5-ACCAGCCACCACCTTCTGATAG-3. The Dorfin transgene copy number in each line was determined by densitometric comparison of the Southern blot hybridization intensity of the DNA with known standards or quantitative real-time RT-PCR using the iCycler system (Bio-Rad, Hercules, CA) as previously described (Ishigaki et al., 2002). Transgenic mice overexpressing human SOD1 carrying a Gly93Ala mutation were obtained from Jackson Laboratories (Bar Harbor, ME). Transgenic progeny were identified by PCR using primers specific for human SOD1 (Gurney et al., 1994). Genotyping of mice was performed by PCR using mouse tail DNA. G93A mutant SOD1 Tg mice were maintained by crossing to F1 of C57BL/6 and SJL. We performed real-time quantitative PCR with mouse tail DNA to estimate the mutant SOD1 copy number in each mouse. We calculated the ratio of mutant SOD1 relative to apolipoprotein B, an internal reference, and compared these results with those of founder mouse tail DNA known to have 25 copies of mutant SOD1 (Dal Canto et al., 1996) using the primer set 5′-CATCAGCCCTAATCCATCTGA-3′ and 5′-CGCGACTAACAATCAAAGTGA-3′ for mutant SOD1 and using the primer set 5′-GGCAAACACTTACGGGTCAT-3′ and 5′-TTGGCTGTTAGAATGCTGGA-3′ for apolipoprotein B. We excluded mice with a low copy number of mutant SOD1. We analyzed the Dorfin transgenic lines 513 and 526 of this mouse model in the present study.

To determine the potential neuroprotective role of Dorfin in ALS, we crossed hemizygous Dorfin Tg mice with hemizygous G93A mutant SOD1 Tg mice. This mating resulted in the generation of four groups of mice: 1) wild type, 2) Dorfin single transgenic mice (Dorfin Tg), 3) G93A single transgenic mice (G93A SOD1 Tg), and 4) Dorfin and G93A SOD1 double transgenic mice (Dorfin/G93A SOD1 double Tg). We compared littermates of G93A SOD1 Tg mice and Dorfin/G93A SOD1 double Tg mice using the following examinations, and we excluded the mice that died of symptoms unrelated to ALS such as injury by fighting each other, difficulty with the water feeding device, and trauma. The mice had ad libitum access to food and water on the bottoms of their cages during the light phase of the 12-hr light/12-hr dark cycle, as described previously (Adachi et al., 2001; Katsuno et al., 2003). All animal experiments were performed in accordance with the National Institutes of Health *Guide for the care and use of laboratory animals* and were approved by the Nagoya University Animal Experiment Committee. All animal experiments were performed with the investigator blinded to genotype.

Assessment of Neurological Phenotype

We assessed the life span of the mice in each group. The end point of survival dates was defined as when an animal could not stand up within 30 sec after it was put on a flat board on both the right and the left sides. Rotarod performance was assessed by using an Economex Rotarod (Columbus Instruments, Columbus, OH). Three trials were performed at 5 rpm, and the longest duration that each mouse remained on the rod was recorded. The timer was stopped when the mouse fell from the rod or after an arbitrary limit of 300 sec.

The footprints of mice were collected as they walked on a straight line. Their front paws were painted with red ink and the hind paws with blue ink. Stride was measured within the area showing regular walking. The longest three strides of both hind paws were measured. Strides of mice that could not walk were measured as zero. Motor activity was analyzed at 10 weeks (presymptomatic stage), 14 weeks (early stage), and 18 weeks (end stage) of age.

Immunohistochemistry

Mice were exsanguinated under ketamine-xylazine anesthesia and transcardially perfused with 20 ml of 4% paraformaldehyde in phosphate buffer (pH 7.4). Tissues were post-fixed overnight in 10% phosphate-buffered formalin and proc-

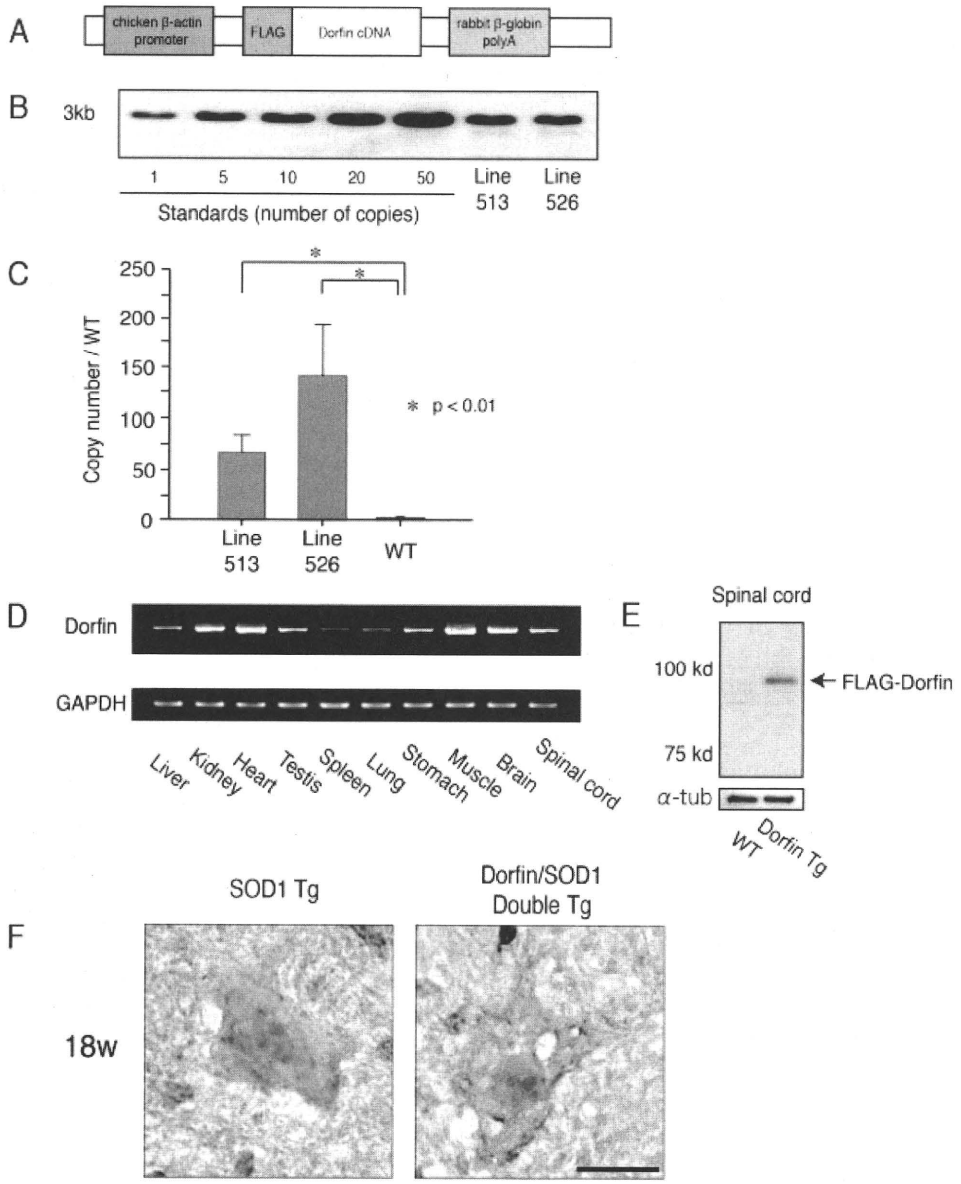

Fig. 1. Dorfin transgenic mouse. **A:** Schematic view of the transgene constructs. The microinjected fragment was composed of a chicken β-actin promoter, a FLAG-tagged Dorfin, and a rabbit β-globin polyadenylation signal sequence (poly-A). **B:** Southern blot analysis of Dorfin transgenic mouse tail DNA. About 20 copies of FLAG-Dorfin transgene are detected in DNA samples from lines 513 and 526. **C:** Quantitative RT-PCR analysis of Dorfin mRNA expression. Total RNA samples were extracted from spinal cord of Dorfin Tg and wt mice (*$P < 0.01$; n = 3 each). Dorfin Tg mice from both lines 513 and 526 express Dorfin mRNA at significantly higher levels than wt mice. Error bars represent SEM. **D:** Transgene expression in Dorfin 526 line Tg mice. RT-PCR analysis of RNA from systemic organs. **E:** Dorfin protein in the spinal cord of 526 Dorfin Tg mouse. Immunoprecipitation using anti-FLAG antibody demonstrates that exogenous FLAG-Dorfin is detected only in Dorfin Tg mice. **F:** Immunohistochemistry of the spinal cord of 526 Dorfin/G93A SOD1 double Tg mice and G93A SOD1 Tg mice with antibodies against Dorfin. Scale bar = 20 μm.

essed for paraffin embedding, as previously described (Adachi et al., 2001; Katsuno et al., 2002). Transverse sections of spinal cord (4 μm thick) were deparaffinized, rehydrated, and treated for antigen retrieval. For the mutant SOD1 immunohistochemical study, the paraffin sections were pretreated with formic acid for 5 min at room temperature; processed using the Ventana Discovery system (Ventana, Tucson, AZ) with heating at 100°C for 30 min; and incubated with mouse anti-SOD1Ab, NCL-SOD1 (1:5,000; Novocastra, Newcastle upon Tyne, United Kingdom), and biotin-SP-conjugated goat anti-mouse IgG (1:500; Jackson Immunoresearch, West Grove, PA) using the Ventana DAB map kit (Ventana, Tucson, AZ). For immunostaining of ubiquitin, sections were similarly processed and incubated with antiubiquitin mouse monoclonal antibody 4PD1 (1:1,000; Santa Cruz Biotechnology, Santa Cruz, CA) and biotin-SP-conjugated goat anti-mouse IgG

(1:500; Jackson Immunoresearch). The areas of SOD1-positive immunoreactivity or ubiquitin-positive aggregates in the anterior horn of transverse spinal cord sections were assessed with a computer-assisted image analyzer (Win roof; Mitani Corporation, Tokyo, Japan) under the light microscope (Axio Imager M1; Carl Zeiss Japan, Tokyo, Japan). Each spinal cord section was divided into four portions by coronal and sagittal lines passing through the central canal. The immunoreactive areas in the gray matter of the above-mentioned dorsal portions were summed and divided by the area of the entire gray matter of the same portion to calculate the ratio of the immunoreactive area. One hundred consecutive transverse sections of the lumbar spinal cord were prepared for each of five mice, and SOD1- or ubiquitin-positive areas in the anterior horn were assessed on every tenth section, as described previously (Terao et al., 1996). For Dorfin immunohistochemistry, we air dried cryostat sections (6 μm thick) of mice spinal cord (Katsuno et al., 2003) and stained them with antiserum against Dorfin (Dorfin-41, 1:200; Niwa et al., 2001; Hishikawa et al., 2003). For double-immunofluorescence staining of the spinal cord, sections were blocked with 4% goat serum and then sequentially incubated with anti-GFAP antibody (1:1,000; Dako, Glostrup, Denmark) and anti-SOD1 antibody (1:100; NCL-SOD1). Anti-GFAP antibody was visualized by anti-rabbit goat IgG coupled with Alexa Fluor 488 (Molecular Probes, Eugene, OR), and anti-SOD1 antibody was visualized with anti-mouse goat IgG coupled with Alexa Fluor 568 (Molecular Probes). Stained sections were observed under an LSM-710 confocal microscope (Carl Zeiss, Gottingen, Germany).

Morphometric Analyses of Spinal Neurons and Ventral Spinal Roots

To assess the neuron populations, 100 serial (4 μm thick) sections from L5 lumbar spinal cords were prepared as described above. Every tenth section was examined by the disector method. The section was stained by the Nissl technique, and neurons in the anterior horn were counted by the disector method using the nucleolus as the leading edge on an Axio vision image analyzer (Carl Zeiss Japan) as described previously (Terao et al., 1996; West, 1999). Data were expressed as the number of neurons per volume of 400 μm thickness of unilateral ventral horn.

The L5 ventral roots were fixed in 2.5% glutaraldehyde in 0.125 M cacodylate buffer (pH 7.4) and embedded in epoxy resin for morphometric analysis. Morphological changes and diameters of myelinated fibers with normal shape were assessed in toluidine blue-stained semithin sections. Morphological changes of myelinated fibers were assessed as described previously (Dyck et al., 1993). Abnormal fibers were those with swollen axons or with a myelin ovoid showing the figure of axonal change (Dyck et al., 1993). Normally shaped myelinated fibers were chosen manually, and their diameters were measured using a computer-assisted image analyzer (Axiovision; Carl Zeiss Japan, Tokyo, Japan), as described previously (Katsuno et al., 2002; Minamiyama et al., 2004). The results were expressed as a diameter frequency histogram per whole L5 ventral root using the data from normally shaped fibers. The ratio of the normally shaped small fibers (<6 μm) and normally shaped large fibers (≥6 μm) to the number of normally shaped fibers at 10 weeks, 14 weeks, and 18 weeks of age were investigated. The ratio of the number of abnormal fibers against the normal and abnormal fibers was examined.

Immunoprecipitation and Western Blotting Analysis

Spinal cords were snap-frozen with powdered CO_2 in acetone (Katsuno et al., 2003). Frozen tissue was homogenized in ice-cold lysis buffer (50 mM HEPES, pH 7.4, 150 mM NaCl, 10 mM EDTA, 1% NP-40), maintained at 4°C for 30 min, and centrifuged at 18,000*g* for 30 min at 4°C. The protein concentration of the supernatant (soluble fraction) was determined by using the DC protein assay (Bio-Rad). The pellet fractions were suspended in ice-cold buffer (0.5% SDS, 8 M urea, 1% β-mercaptoethanol, 50 mM phosphate buffer, pH 7. 4), homogenized 15 times, and kept at 4°C for 30 min. Samples were then centrifuged at 18,000*g* for 30 min at 4°C to obtain the supernatant (insoluble fraction).

Immunoprecipitation from the soluble fraction was performed with 8 μg anti-FLAG rabbit antibody (Sigma, St. Louis, MO) and Protein A/G Plus-Agarose (Santa Cruz Biotechnology), and the precipitates were washed four times. Spinal cord lysates or immunoprecipitates were separated by SDS-PAGE (5–20% gradient gel). Western blotting was performed using standard procedures as described previously (Katsuno et al., 2002; Minamiyama et al., 2004). Primary antibodies were used at the following concentrations: anti-FLAG M2, 1:1,000 (Sigma); anti-Cu-Zn SOD1, 1:5,000 (SOD-100; Stressgen, Victoria, British Columbia, Canada); anti-Dorfin, 1:1,000 (Dorfin 30; Hishikawa et al., 2003). Secondary antibody probing and detection were performed using the ECL Plus kit (GE Healthcare, Buckinghamshire, United Kingdom). Chemiluminescence signals were digitalized (LAS-3000 Imaging System; Fujifilm, Tokyo, Japan), and band intensities were quantified in Multi Gauge software version 3.0 (Fujifilm).

Statistical Analyses

Data were analyzed by Kaplan-Meier and log-rank tests for survival rate, unpaired *t*-tests for the results of RT-PCR, two-factor repeated measure ANOVA for the Rotarod and footprint, one-factor factorial ANOVA with Fisher's probability of least significant differences post hoc test for the results of immunohistochemical study with SOD1 and ubiquitin antibody, and two-factor factorial ANOVA for the other analyses (Statview version 5; Hulinks, Tokyo, Japan). *P* values of 0.05 or less denoted statistical significance.

RESULTS

Dorfin Transgenic Mice

We established 20 lines of Dorfin transgenic mice and examined 10 different organs for exogenous, FLAG-tagged Dorfin mRNA expression. We assessed the number of copies of Dorfin transgene in each Dorfin Tg mouse line by Southern blotting (Fig. 1B) and quantitative RT-PCR (Fig. 1C) and selected two Dorfin Tg mouse lines for further study (513 and 526). Approximately 20 copies of the FLAG-Dorfin transgene were

TABLE I. Copy Number of Mutant SOD1 Gene*

Genotype	G93A mutant SOD1 copy number
Dorfin/G93A mSOD1 double Tg	25.2 ± 1.6
G93A mSOD1 Tg	25.0 ± 1.1

*Values are the mean ± SD, n = 72 (Dorfin/G93A mSOD1 double Tg), n = 77 (G93A mSOD1 Tg).

detected in DNA samples from each of these lines. Exogenous Dorfin was highly expressed in the spinal cord, brain, muscles, kidney, heart, and testis and was not substantially detected in the stomach, lung, spleen, or liver (Fig. 1D). We were unable to detect the exogenous Dorfin protein by Western blotting, probably because of its short half-life (Ishigaki et al., 2007). Immunoprecipitation using anti-FLAG antibody showed that exogenous Dorfin protein was detected only in the Dorfin Tg mice (Fig. 1E). We also detected Dorfin protein by immunohistochemistry with Dorfin antibody in Dorfin/G93A SOD1 double Tg mouse spinal cord sections (Fig.1F). We did not find differences in size, body weight, gross morphology, or behavior between the Dorfin Tg mice and their littermates, indicating that Dorfin overexpression does not affect normal mouse development.

Dorfin Ameliorates Clinical Phenotypes in a Transgenic Mouse Model of ALS

To determine the potential neuroprotective role of Dorfin in mutant SOD1-related ALS, progeny of Dorfin transgenic mice (lines 513 and 526) were crossed with G93A mutant SOD1 transgenic mice [B6SJL-TgN (SOD1-G93A)1Gur] (Gurney et al., 1994). The mean copy number of the mutant SOD1 gene in mice used for examinations is shown in Table I. The same copy number was observed in Dorfin/G93A SOD1 double Tg mice and G93A SOD1 Tg mice. We determined the life span and assessed motor impairment in both lines of Dorfin/G93A SOD1 double Tg mice and G93A SOD1 Tg mice. Dorfin/G93A SOD1 double Tg mice survived significantly longer than SOD1 Tg offspring from crossings of either Dorfin Tg line (Fig. 2A). Dorfin improved the mean survival time (513 Dorfin/G93ASOD1 double Tg at 144.9 days vs. G93ASOD1 Tg at 134.4 days, $P < 0.01$; and 526 Dorfin/G93ASOD1 double Tg at 142.2 days vs. G93ASOD1 Tg at 131.7 days, $P < 0.01$) as well as the maximal life span (513 Dorfin/G93ASOD1 Double Tg at 175 days vs. G93A SOD1 Tg at 155 days and 526 Dorfin/G93ASOD1 Double Tg at 167 days vs. G93A SOD1 Tg at 148 days; Fig. 2A). Both Dorfin Tg lines showed a significant increase in the mean life span of approximately 10 days and a significant increase in maximal life span of approximately 20 days. As a measure of motor impairment, we assessed Rotarod performance and foot stride during walking. The onset of motor impairment on the Rotarod task was delayed for 1 week in both lines of Dorfin/G93A SOD1 double Tg mice, and the progression of the motor deficit was slowed by 1–2 weeks compared with that observed in the G93A SOD1 Tg mice. Both the 513 and the 526 lines of Dorfin/G93A SOD1 double Tg mice performed significantly better than the G93A SOD1 Tg mice ($P < 0.05$, ANOVA; Fig. 2B; 513: Dorfin/G93ASOD1 double Tg 300 ± 0.0 sec vs. G93ASOD1 Tg 300 ± 0.0 sec at 10 weeks of age, 300 ± 0.0 sec vs. 278.8 sec at 14 weeks of age, 160.8 ± 34.2 sec vs. 67.8 ± 25.5 sec at 18 weeks of age; 526: 300 ± 0.0 sec vs. 300 ± 0.0 sec at 10 weeks of age, 300 ± 0.0 sec vs. 300 ± 0.0 sec at 14 weeks of age, 135.8 ± 29.8 sec vs. 86.0 ± 27.0 sec at 18 weeks of age). We analyzed the walking strides at three time points, 10 weeks (presymptomatic stage), 14 weeks (early stage), and 18 weeks of age (end stage). Both lines of Dorfin/G93ASOD1 double Tg mice showed significantly longer foot strides than the G93A SOD1 Tg mice (513: $P < 0.05$; 526: $P < 0.01$, ANOVA; Fig. 2C; 513: Dorfin/G93ASOD1 double Tg 68.0 ± 2.0 mm vs. G93ASOD1 Tg 63.0 ± 0.9 mm at 10 weeks of age, 69.7 ± 2.3 mm vs. 63.6 ± 0.9 mm at 14 weeks of age, 29.9 ± 5.8 mm vs. 20.1 ± 3.0 mm at 18 weeks of age; 526: 67.3 ± 1.8 mm vs. 67.1 ± 0.9 mm at 10 weeks of age, 63.1 ± 1.3 mm vs. 63.3 ± 1.4 mm at 14 weeks of age, 50.1 ± 5.6 mm vs. 26.0 ± 4.5 mm at 18 weeks of age).

Dorfin Ameliorates Histopathological Changes in the Transgenic Mouse Model of ALS

Dorfin ameliorated histopathological impairments in spinal neurons (Fig. 3A) and their axons in the double Tg mice (Fig. 3B). We assessed the size of the neuron population in the lumbar spinal cord and the distribution of ventral root diameters. The number of neurons in the unilateral lumbar spinal anterior horn was significantly larger in the Dorfin 526/G93ASOD1 double Tg mice than in the G93ASOD1 Tg mice examined with ANOVA ($P < 0.05$; n = 5). Dorfin overexpression also ameliorated histopathological changes in the ventral roots. Histograms of the diameters of myelinated fibers in the G93ASOD1 Tg mouse lumbar ventral roots showed decreases in the numbers of large myelinated fibers with age, whereas the 526 Dorfin/G93ASOD1 double Tg mice retained these large axons even at 18 weeks of age (Fig. 3B). We investigated the ratio of normally shaped small myelinated fibers (<6 μm) and normally shaped large myelinated fibers (≥6 μm) to the normally shaped fibers (Fig. 3C), and the ratio of abnormally shaped fibers to the normally shaped and abnormally shaped fibers (Fig. 3D) at 10 weeks, 14 weeks, and 18 weeks of age with ANOVA. Dorfin/G93ASOD1 double Tg mice showed a significantly lower ratio of small myelinated fibers ($P < 0.05$, ANOVA) and a higher ratio of large myelinated fibers ($P < 0.05$, ANOVA) compared with G93A SOD1 Tg mice. The ratio of abnormal fibers in Dorfin/G93ASOD1 double Tg mice was significantly lower than that of G93ASOD1 Tg mice ($P < 0.05$, ANOVA).

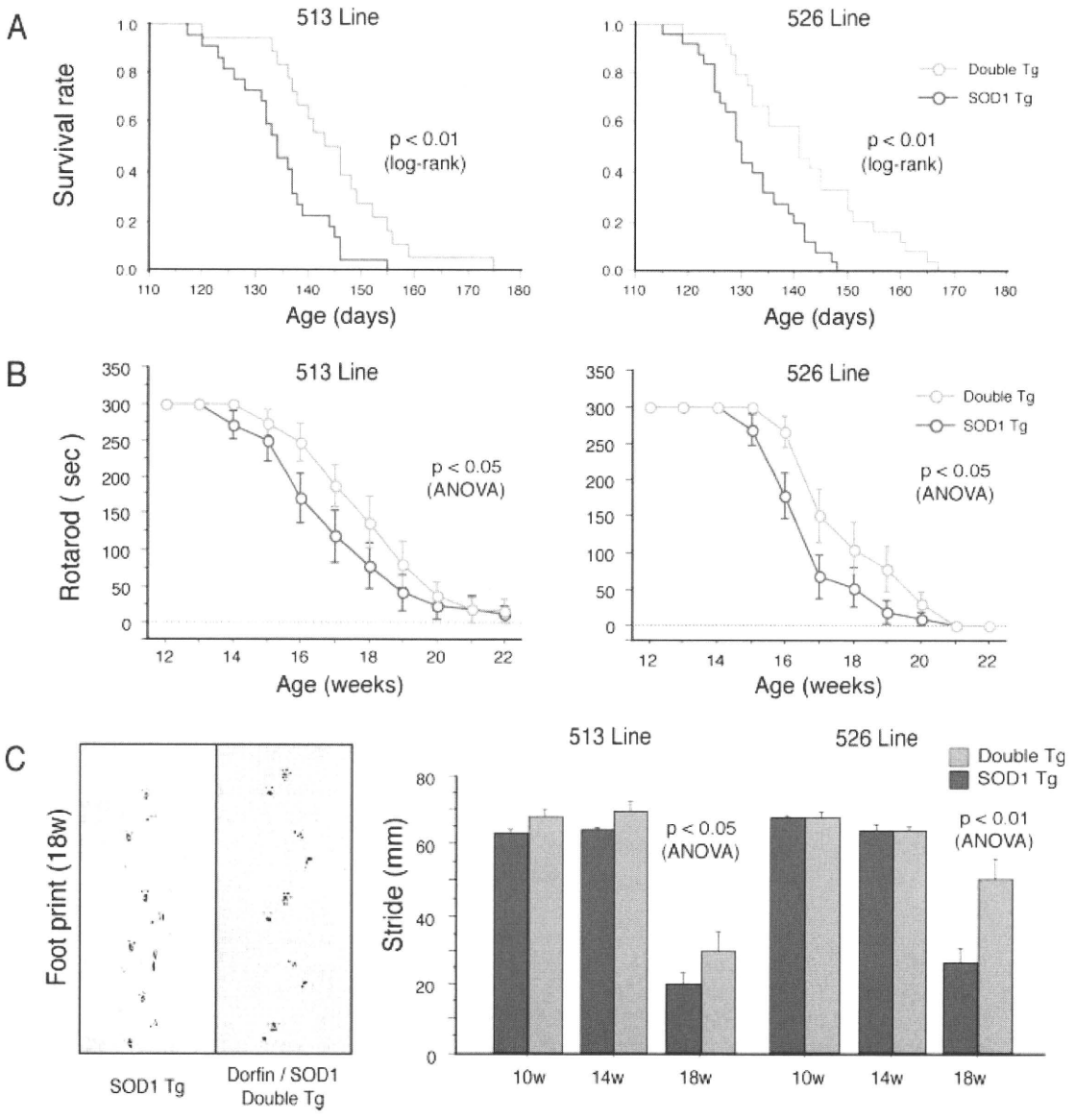

Fig. 2. Dorfin ameliorates clinical phenotypes of G93A mutant SOD1 Tg mice. **A:** Survival rate (Kaplan-Meier). Dorfin/G93A SOD1 double Tg mice of both lines 513 and 526 (green) show significantly longer survival times than the G93A SOD1 Tg mice ($P < 0.01$ log-rank). **B:** Rotarod task. Both 513 and 526 lines of Dorfin/G93A SOD1 double Tg mice perform significantly better on the Rotarod task than the G93A SOD1 Tg mice ($P < 0.05$, ANOVA). **C:** Left: Footprints of 526 line mice at 18 weeks of age. Front paws are in red and hind paws in blue. Right: Dorfin/G93A SOD1 double Tg mice of both lines show longer strides than the G93A SOD1 Tg mice (513: $P < 0.05$, 526: $P < 0.01$, ANOVA). The number of mice was 513 line: n = 18 (male = 10, female = 8) in Dorfin/G93ASOD1 double Tg and n = 22 (male = 8, female = 14) in G93A SOD1 Tg; 526 line: n = 24 (male = 12, female = 12) in Dorfin/G93ASOD1 double Tg and n = 25 (male = 9, female = 16) in G93A SOD1 Tg. Values represents means ± SEM.

Dorfin Decreases the Amount of Mutant SOD1 in the Spinal Cord of SOD1 Tg Mice

As we reported previously (Niwa et al., 2002), the overexpression of Dorfin accelerated the degradation of mutant SOD1 protein by the ubiquitin-proteasome system. We investigated the ability of Dorfin to reduce the amount of mutant SOD1 protein using immunohistochemistry at 18 weeks of age and Western blotting of mice spinal cords from line 526 mice (Figs. 4, 5). In transverse sections of the ventral horn (Fig. 4A), the SOD1-positive areas from Dorfin/G93ASOD1 double Tg mice were significantly smaller than those in G93ASOD1 Tg mice (Fig. 4B; Dorfin/G93ASOD1 double Tg at 2.66% vs. G93ASOD1 Tg at 3.45%, $P < 0.01$). Immunohistochemistry with antiubiquitin antibody revealed that ubiquitin-positive protein accumulations were present in the cytoplasm of the residual motor neurons and also in the neuropil (Fig. 4C). The

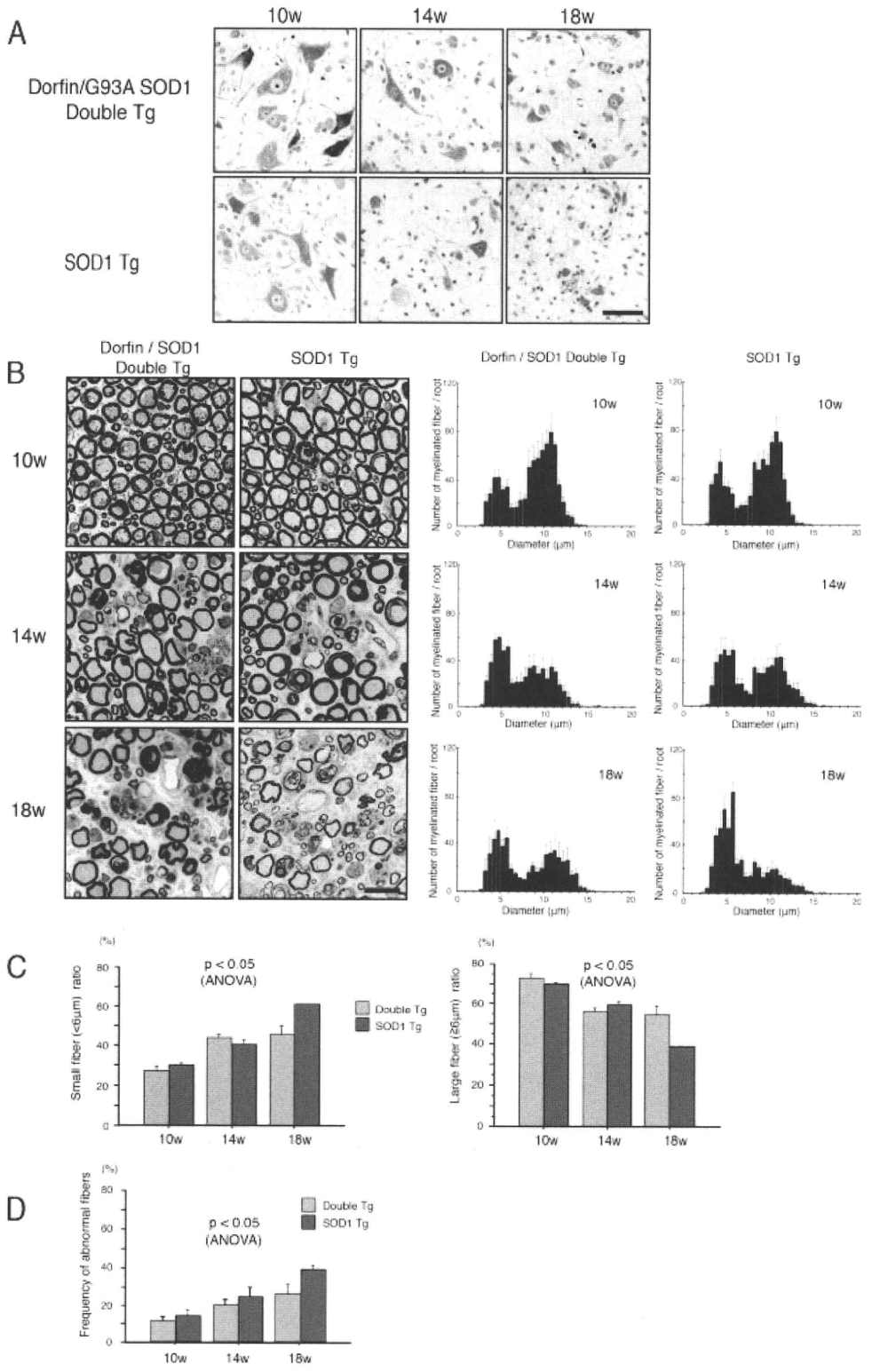

Fig. 3. Histopathological analysis of spinal cord and ventral roots of 526 Dorfin/G93A mutant SOD1 double Tg mice and G93A mutant SOD1 Tg mice. **A:** Transverse section of Nissl-stained L5 spinal anterior horns of 526 Dorfin/G93A mutant SOD1 double Tg mice and G93A mutant SOD1 Tg mice at 10 weeks, 14 weeks, and 18 weeks of age. **B:** Transverse, semithin section of L5 ventral roots stained with toluidine blue at 10 weeks, 14 weeks, and 18 weeks of age. Histograms of the diameters of myelinated fibers in the ventral roots show that the progressive decrease in the number of large myelinated fibers was suppressed in Dorfin/G93A SOD1 double Tg mice compared with G93A SOD1 Tg mice at 18 weeks (n = 3). **C:** Bar graphs of the small fiber ratio (%) of the ventral root ($P < 0.05$, ANOVA) and bar graphs of the large fiber ratio (%) of the ventral root ($P < 0.05$, ANOVA). **D:** The frequency of abnormal fibers. Dorfin/G93A SOD1 double Tg mice show a significantly lower frequency of abnormal fibers than G93A SOD1 Tg mice ($P < 0.05$, ANOVA). Scale bars = 50 μm in A; 20 μm in B. [Color figure can be viewed in the online issue, which is available at www.interscience.wiley.com.]

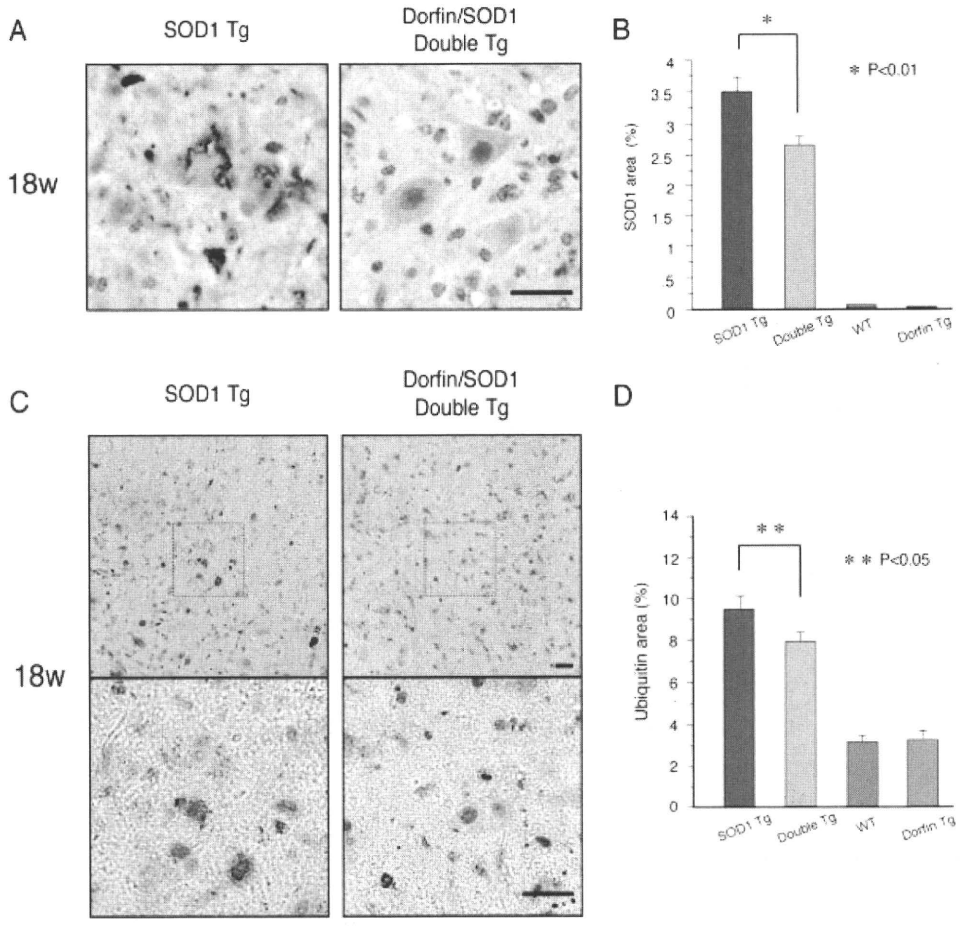

Fig. 4. Dorfin/G93A SOD1 double Tg mice show a decreased amount of mutant SOD1 protein and ubiquitin-positive aggregates under overexpression of Dorfin. Immunohistochemistry of the spinal cord of 526 Dorfin/G93A SOD1 double Tg mice and G93A SOD1 Tg mice with antibodies against SOD1 (**A**), ubiquitin (**C**; low magnification in upper column; square indicates the area magnified in high magnification in lower column). Bar graphs of the relative sizes of SOD1-positive (**B**) and ubiquitin-positive (**D**) areas in the L5 spinal anterior horn at 18 weeks of age compared with the total areas of gray matter. $*P < 0.01$, $**P < 0.05$. WT, wild-type mice, Dorfin Tg;, dorfin Tg mice. Scale bars = 20 μm.

accumulations of ubiquitin-positive proteins were less in the Dorfin/G93A SOD1 double Tg mice than in the G93A SOD1 Tg mice (Fig. 4D; Dorfin/G93ASOD1 double Tg at 7.99% vs. G93ASOD1 Tg at 9.56%, $P < 0.05$).

Glial Pathology in the Spinal Cord of Tg Mice

We investigated the glial cell pathology using anti-GFAP antibody. The findings from confocal microscopy showed no striking differences in the degree of gliosis between SOD1 Tg and Dorfin/SOD1 double Tg mice (Fig. 5). Double immunofluorescence staining showed that SOD1-positive inclusion was not observed in the cytoplasm of astrocytes in the spinal cords of both SOD1 Tg and Dorfin/SOD1 double Tg mice.

Western Blot Analysis in the Spinal Cord of Tg Mice

Results from Western blotting analysis showed that the level of mutant SOD1 in the soluble fraction of spinal cord from the Dorfin/G93A double Tg mice was significantly less than that of spinal cord from the G93ASOD1 Tg mice (Fig. 6A; $P < 0.01$ ANOVA). The decrease in SOD1 levels was most prominent at 18 weeks of age. We observed the same tendency in the insoluble fraction, but the decrease was not significant (Fig. 6B; ANOVA). These decreases of mutant SOD1 proteins were observed under Dorfin overexpression (Fig. 1F).

DISCUSSION

Recently, several E3s, including Dorfin, were identified that specifically recognize and reduce the levels of mutant SOD1 protein in an in vitro cell culture model (Niwa et al., 2002; Miyazaki et al., 2004; Urushitani et al., 2004). However, these results have not been verified in vivo. In the present study, we demonstrated for the first time that transgenically overexpressed Dorfin, as an E3, attenuates the accumulation of mutant SOD1 deposition, reduces neuronal death and axonal degenera-

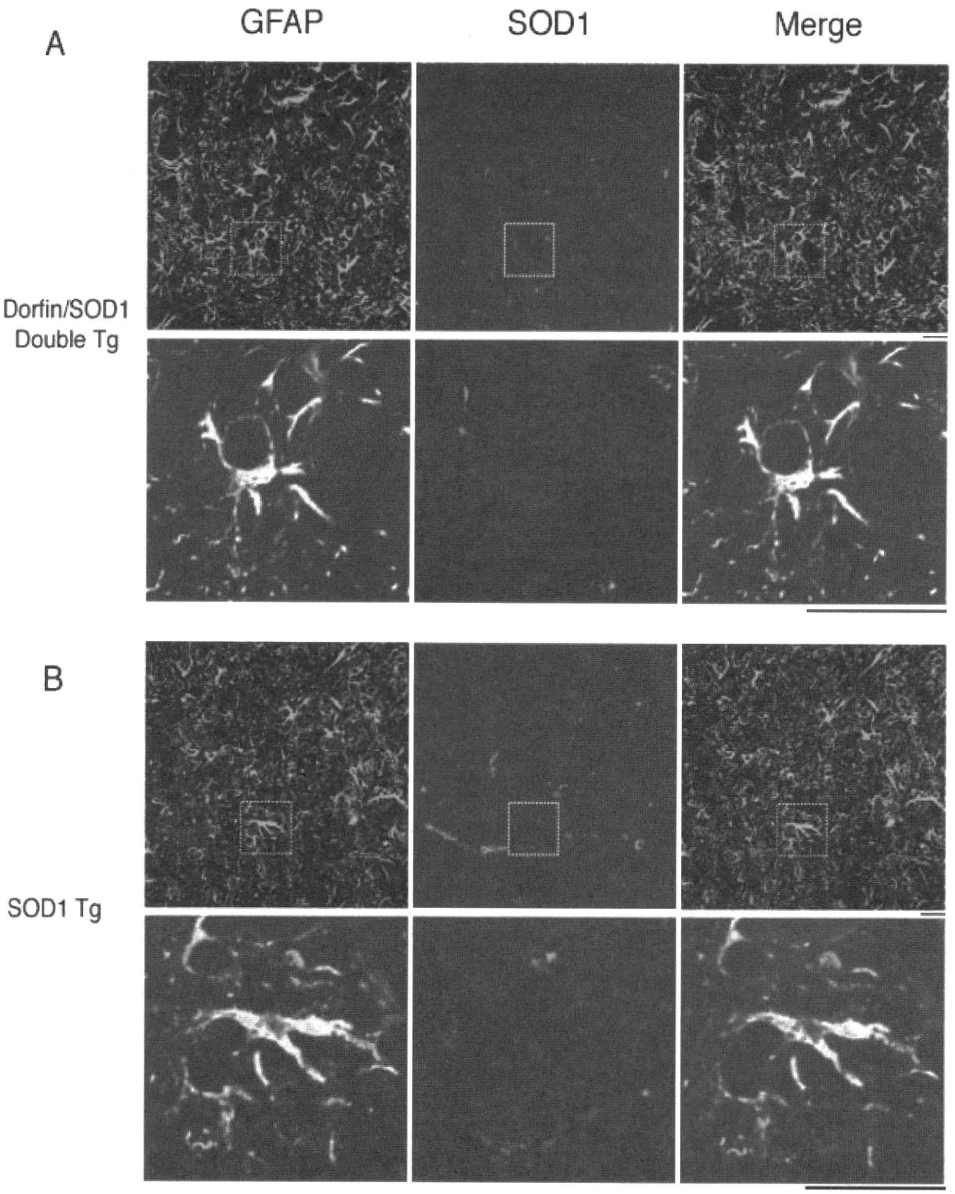

Fig. 5. Imunofluorescence study of the spinal cord of 526 Dorfin/G93A SOD1 double Tg mice (**A**) and G93A SOD1 Tg mice (**B**) using antibodies against GFAP and SOD1. Low magnification at upper column and high magnification in lower column (The square indicates the area magnified in high magnification in lower column). The findings revealed no striking differences in the degree of gliosis between SOD1 Tg and Dorfin/SOD1 double Tg. SOD1 protein was not localized in astrocytes. Scale bars = 20 μm.

tion of motor neurons, ameliorates motor performance deficits, and extends the life span of G93A SOD1 transgenic mice.

The E3 CHIP was reported to degrade toxic misfolded proteins associated with molecular chaperons Hsp70 and Hsp90 (McDonough and Patterson, 2003; Shin et al., 2005; Dickey et al., 2006) and to ameliorate the phenotypes of transgenic mouse (Adachi et al., 2007) and zebrafish (Miller et al., 2005) models of polyglutamine disease. These reports suggest that the overexpression of this E3 is beneficial for rescuing the phenotype of neurodegenerative disease.

As opposed to CHIP, Dorfin specifically recognizes mutant SOD1 molecules and degrades them via the ubiquitin-proteasome system (Niwa et al., 2001, 2002). This specific recognition suggests an advantage for using Dorfin as a therapeutic tool against mutant SOD1-mediated ALS.

SALS, FALS, and G93A mutant SOD1 Tg mice have been reported to present ubiquitin-positive aggregation (Murayama et al., 1990; Watanabe et al., 2001; Ardley and Robinson, 2004). In this study, we demonstrated a reduction in mutant SOD1 protein and ubiquitin-positive protein accumulation in the spinal cord

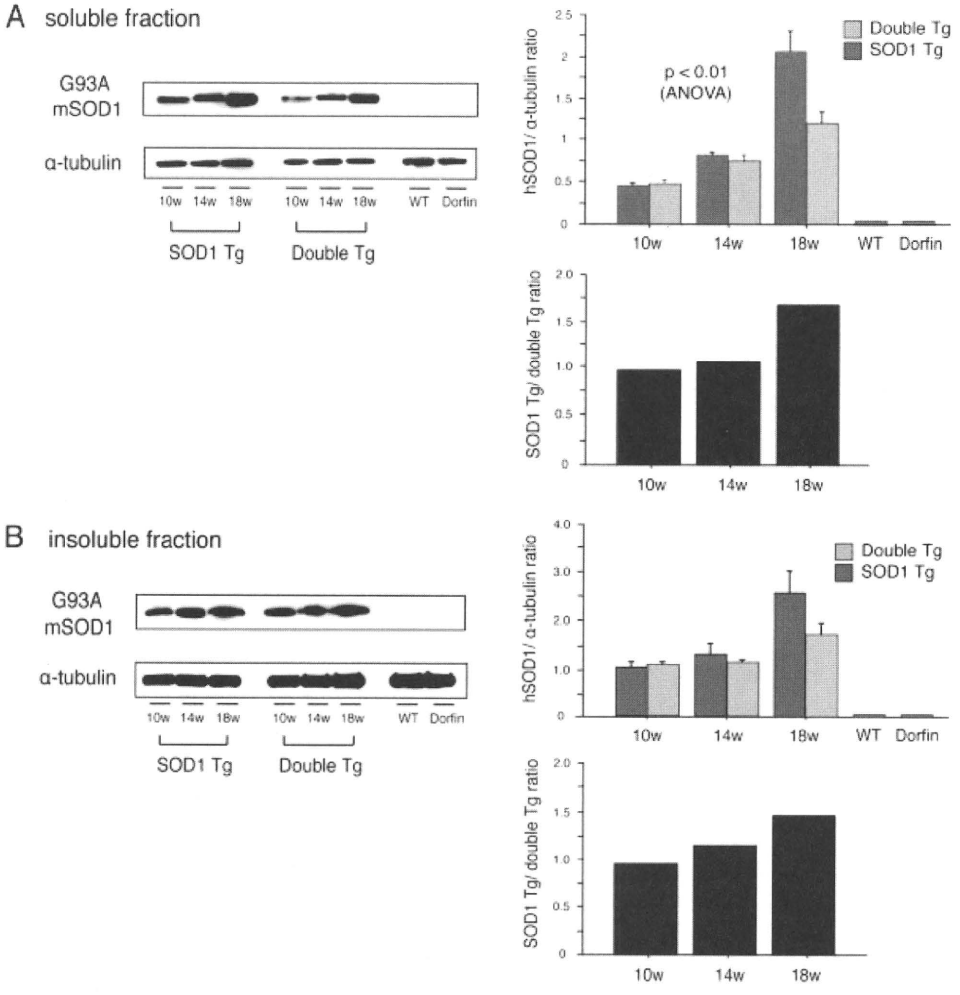

Fig. 6. Western blot analysis of the spinal cord protein extracts from 526 Dorfin/G93A SOD1 double Tg mice and G93A SOD1 Tg mice. Western blotting was performed at 10, 14, and 18 weeks of age using anti-Cu-Zn SOD1 antibody. Soluble fraction (**A**), insoluble fraction (**B**). Each lane contains 10 μg protein. Bar graphs in each case represent the densitometric analysis of the standardized amount of SOD1 protein against endogenous α-tubulin in each Western blot and the ratio of SOD1 Tg/Dorfin/SOD1 double Tg standardized data of at each age. Protein samples were prepared from each of five different mice and averaged in the quantification. Error bars represent SEM. WT, wild-type littermate; Dorfin, dorfin Tg. [Color figure can be viewed in the online issue, which is available at www.interscience.wiley.com.]

resulting from Dorfin overexpression. On Western blots, the reduction of mutant SOD1 was more marked in the soluble fraction from end-stage mice than in the insoluble fraction. Thus, Dorfin overexpression may reduce more soluble mutant SOD1 protein. Dorfin also reduced the histopathological deposition of mutant SOD1 and ubiquitin-positive protein in the spinal cord at 18 weeks of age. Overaccumulation of ubiquitinated, misfolded proteins may adversely affect the proteasome machinery and impair normal protein degradation (Boillee et al., 2006). Thus, a reduction of this deposition may lead to reduced cytotoxicity of spinal neurons and, finally, to the amelioration of histopathological and clinical phenotypes.

These results were consistent with those of our previous study showing that Dorfin overexpression protected against the toxic effects of mutant SOD1 in neuronal cell culture (Niwa et al., 2002). Dorfin overexpression reduced the levels of mutant SOD1 by recognizing and ubiquitinating mutant SOD1 proteins and by targeting them for proteasomal degradation, thereby protecting against neuronal cell death (Niwa et al., 2002, 2007).

Histopathological amelioration as assessed by observing the number of neurons in the anterior horn and ventral root was detected. The number of abnormal fibers was decreased, and the population of large fibers was well preserved in Dorfin/G93A SOD1 double Tg mice compared with G93A SOD1 Tg mice. From these results, we infer that Dorfin overexpression has a protective effect against axonal degeneration caused by G93A mutant SOD1 protein. These histopathological ameliorations may lead to the improvement of clinical phenotypes as indicated by improvements in the Rotarod tasks and foot strides reported here, although there was no

remarkable difference in the degree of gliosis in the spinal cords. Many reports have suggested that not only motor neurons but also other cell types, such as astrocytes, play an important role in neurodegeneration (Pramatarova et al., 2001; Clement et al., 2003; Boillee et al., 2006). In our examination, we observed that SOD1 positive aggregates existed in the cell body of neurons, but there were no aggregates observed in astrocytes from either G93A SOD1 Tg or Dorfin/SOD1 double Tg mice. This result suggests that the overexpressed Dorfin was unable to ubiquitinate G93A mutant SOD1 protein in the astrocytes because there was no accumulation of G93A mutant SOD1 protein in the astrocytes of G93A SOD1 Tg mice. Consequently, Dorfin may have no beneficial effect on the astrocyte cell function impaired by mutant SOD1 protein.

Although many hypotheses for the pathogenesis of ALS have been proposed (Julien, 2001; Boillee et al., 2006; Kabashi and Durham, 2006; Van Deerlin et al., 2008), we suggest that a reduction in the levels of mutant SOD1 may have a beneficial effect on neuronal cell viability, including mitochondria function and a potential for therapeutic use (Niwa et al., 2002; Takeuchi et al., 2004).

In the present study, Dorfin overexpression was effective in ameliorating the ALS phenotypes of the G93A SOD1 Tg mouse but was not as efficient as treatment with VEGF or IGF-1 delivered via the lentivirus system (Kaspar et al., 2003; Azzouz et al., 2004). One reason for this reduced efficacy may be that transgenically expressed Dorfin does not clear sufficient amounts of mutant SOD1 protein to eliminate the phenotypes because of its short half-life (Ishigaki et al., 2007). Dorfin may be precisely regulated in its expression level in vivo, and, thus, exogenously expressed human Dorfin under the β-actin promoter may be degraded immediately. Moreover, as the pathology of the G93A SOD1 mouse progresses, the function of the proteasome gradually deteriorates (Kabashi et al., 2004; Cheroni et al., 2005; Boillee et al., 2006; Cheroni et al., 2009), and Dorfin may lose its E3 activity to clear the mutant SOD1 with advancing disease. Strategies to improve the activity of Dorfin include the utilization of a Dorfin-CHIP chimeric protein, which has the E3 activity of Dorfin and a longer half-life, as we reported previously (Ishigaki et al., 2007), and, alternatively, the crossing of the Dorfin Tg mouse with other mutant SOD1 Tg mouse showing milder symptoms with a slower progressive course than G93A. In these cases, Dorfin may exert a more marked amelioration of the phenotypes. In the present study, the gender balance of the mice was different to some extent between Dorfin/SOD1 double Tg and SOD1 Tg in both the 513 and the 526 lines (percentage of male mice 513: 55% for Dorfin/SOD1 double Tg, 36.3% for SOD1 Tg; 526: 50% for Dorfin/SOD1 double Tg, 36% for SOD1 Tg). The differences in SOD1 Tg motor function and survival between males and females has been reported previously (Mahoney et al., 2004; Stam et al., 2008). Female mice showed a longer survival and better motor function, and the difference of gender balance may contribute to a modest difference of survival or motor function.

The important point of this study is that the overexpression of a toxic protein-specific E3 that reacts specifically and directly with mutant SOD1 ameliorated the clinical and pathological phenotypes of mutant SOD1-mediated motor neuron degeneration. Dorfin has been shown in previous studies to localize to various inclusions found in neurological tissue samples of human disease. For SALS, the Lewy body-like inclusions were immunoreactive for anti-Dorfin antibody, and, for FALS, the hyaline-like inclusions were positive for Dorfin (Hishikawa et al., 2003; Ito et al., 2003). These findings suggest that Dorfin may be involved in the pathogenesis of a broad spectrum of neurodegenerative disorders (Hishikawa et al., 2003; Ito et al., 2003) and may provide a clue to the treatment of these diseases. The activation or induction of the E3 Dorfin may be an effective therapeutic strategy for a wide range of neurodegenerative diseases.

REFERENCES

Adachi H, Kume A, Li M, Nakagomi Y, Niwa H, Do J, Sang C, Kobayashi Y, Doyu M, Sobue G. 2001. Transgenic mice with an expanded CAG repeat controlled by the human AR promoter show polyglutamine nuclear inclusions and neuronal dysfunction without neuronal cell death. Hum Mol Genet 10:1039–1048.

Adachi H, Waza M, Tokui K, Katsuno M, Minamiyama M, Tanaka F, Doyu M, Sobue G. 2007. CHIP overexpression reduces mutant androgen receptor protein and ameliorates phenotypes of the spinal and bulbar muscular atrophy transgenic mouse model. J Neurosci 27:5115–5126.

Alves-Rodrigues A, Gregori L, Figueiredo-Pereira ME. 1998. Ubiquitin, cellular inclusions and their role in neurodegeneration. Trends Neurosci 21:516–520.

Ardley HC, Robinson PA. 2004. The role of ubiquitin-protein ligases in neurodegenerative disease. Neurodegen Dis 1:71–87.

Azzouz M, Ralph GS, Storkebaum E, Walmsley LE, Mitrophanous KA, Kingsman SM, Carmeliet P, Mazarakis ND. 2004. VEGF delivery with retrogradely transported lentivector prolongs survival in a mouse ALS model. Nature 429:413–417.

Boillee S, Vande Velde C, Cleveland DW. 2006. ALS: a disease of motor neurons and their nonneuronal neighbors. Neuron 52:39–59.

Bruijn LI, Houseweart MK, Kato S, Anderson KL, Anderson SD, Ohama E, Reaume AG, Scott RW, Cleveland DW. 1998. Aggregation and motor neuron toxicity of an ALS-linked SOD1 mutant independent from wild-type SOD1. Science 281:1851–1854.

Cassina P, Cassina A, Pehar M, Castellanos R, Gandelman M, de Leon A, Robinson KM, Mason RP, Beckman JS, Barbeito L, Radi R. 2008. Mitochondrial dysfunction in SOD1G93A-bearing astrocytes promotes motor neuron degeneration: prevention by mitochondrial-targeted antioxidants. J Neurosci 28:4115–4122.

Cheroni C, Peviani M, Cascio P, Debiasi S, Monti C, Bendotti C. 2005. Accumulation of human SOD1 and ubiquitinated deposits in the spinal cord of SOD1G93A mice during motor neuron disease progression correlates with a decrease of proteasome. Neurobiol Dis 18:509–522.

Cheroni C, Marino M, Tortarolo M, Veglianese P, De Biasi S, Fontana E, Zuccarello LV, Maynard CJ, Dantuma NP, Bendotti C. 2009. Functional alterations of the ubiquitin-proteasome system in motor neurons of a mouse model of familial amyotrophic lateral sclerosis. Hum Mol Genet 18:82–96.

Ciechanover A. 2005. Intracellular protein degradation: from a vague idea thru the lysosome and the ubiquitin-proteasome system and onto human diseases and drug targeting. Cell Death Differ 12:1178–1190.

Clement AM, Nguyen MD, Roberts EA, Garcia ML, Boillee S, Rule M, McMahon AP, Doucette W, Siwek D, Ferrante RJ, Brown RH Jr, Julien JP, Goldstein LS, Cleveland DW. 2003. Wild-type nonneuronal cells extend survival of SOD1 mutant motor neurons in ALS mice. Science 302:113–117.

Dal Canto MC, Mourelatos Z, Gonatas NK, Chiu A, Gurney ME. 1996. Neuropathological changes depend on transgene copy numbers in transgenic mice for mutant human Cu, Zn superoxide dismutase (SOD). In: Nakano I, Hirano A, editors. Amyotrophic lateral sclerosis: progress and perspectives in basic research and clinical application. Amsterdam: Elsevier Science. p 331–338.

Dickey CA, Yue M, Lin WL, Dickson DW, Dunmore JH, Lee WC, Zehr C, West G, Cao S, Clark AM, Caldwell GA, Caldwell KA, Eckman C, Patterson C, Hutton M, Petrucelli L. 2006. Deletion of the ubiquitin ligase CHIP leads to the accumulation, but not the aggregation, of both endogenous phospho- and caspase-3-cleaved tau species. J Neurosci 26:6985–6996.

Dyck PJ, Giannini C, Lais A. 1993. Pathologic alterations of nerves. In: Dyck PJ, Thomas PK, Griffin JW, Low PA, Poduslo JF, editors. Peripheral neuropathy, 3rd ed. Philadelphia: W.B. Saunders. p 514–595.

Goldberg AL. 2003. Protein degradation and protection against misfolded or damaged proteins. Nature 426:895–899.

Gurney ME, Pu H, Chiu AY, Dal Canto MC, Polchow CY, Alexander DD, Caliendo J, Hentati A, Kwon YW, Deng HX, et al. 1994. Motor neuron degeneration in mice that express a human Cu,Zn superoxide dismutase mutation. Science 264:1772–1775.

Hirano A. 1996. Neuropathology of ALS: an overview. Neurology 47(Suppl 2):S63–S66.

Hishikawa N, Niwa J, Doyu M, Ito T, Ishigaki S, Hashizume Y, Sobue G. 2003. Dorfin localizes to the ubiquitylated inclusions in Parkinson's disease, dementia with Lewy bodies, multiple system atrophy, and amyotrophic lateral sclerosis. Am J Pathol 163:609–619.

Ishigaki S, Liang Y, Yamamoto M, Niwa J, Ando Y, Yoshihara T, Takeuchi H, Doyu M, Sobue G. 2002. X-Linked inhibitor of apoptosis protein is involved in mutant SOD1-mediated neuronal degeneration. J Neurochem 82:576–584.

Ishigaki S, Niwa J, Yamada S, Takahashi M, Ito T, Sone J, Doyu M, Urano F, Sobue G. 2007. Dorfin-CHIP chimeric proteins potently ubiquitylate and degrade familial ALS-related mutant SOD1 proteins and reduce their cellular toxicity. Neurobiol Dis 25:331–341.

Ito T, Niwa J, Hishikawa N, Ishigaki S, Doyu M, Sobue G. 2003. Dorfin localizes to Lewy bodies and ubiquitylates synphilin-1. J Biol Chem 278:29106–29114.

Julien JP. 2001. Amyotrophic lateral sclerosis. unfolding the toxicity of the misfolded. Cell 104:581–591.

Kabashi E, Durham HD. 2006. Failure of protein quality control in amyotrophic lateral sclerosis. Biochim Biophys Acta 1762:1038–1050.

Kabashi E, Agar JN, Taylor DM, Minotti S, Durham HD. 2004. Focal dysfunction of the proteasome: a pathogenic factor in a mouse model of amyotrophic lateral sclerosis. J Neurochem 89:1325–1335.

Kabuta T, Suzuki Y, Wada K. 2006. Degradation of amyotrophic lateral sclerosis-linked mutant Cu,Zn-superoxide dismutase proteins by macroautophagy and the proteasome. J Biol Chem 281:30524–30533.

Kaspar BK, Llado J, Sherkat N, Rothstein JD, Gage FH. 2003. Retrograde viral delivery of IGF-1 prolongs survival in a mouse ALS model. Science 301:839–842.

Katsuno M, Adachi H, Kume A, Li M, Nakagomi Y, Niwa H, Sang C, Kobayashi Y, Doyu M, Sobue G. 2002. Testosterone reduction prevents phenotypic expression in a transgenic mouse model of spinal and bulbar muscular atrophy. Neuron 35:843–854.

Katsuno M, Adachi H, Doyu M, Minamiyama M, Sang C, Kobayashi Y, Inukai A, Sobue G. 2003. Leuprorelin rescues polyglutamine-dependent phenotypes in a transgenic mouse model of spinal and bulbar muscular atrophy. Nat Med 9:768–773.

Mahoney DJ, Rodriguez C, Devries M, Yasuda N, Tarnopolsky MA. 2004. Effects of high-intensity endurance exercise training in the G93A mouse model of amyotrophic lateral sclerosis. Muscle Nerve 29:656–662.

Martin LJ, Liu Z, Chen K, Price AC, Pan Y, Swaby JA, Golden WC. 2007. Motor neuron degeneration in amyotrophic lateral sclerosis mutant superoxide dismutase-1 transgenic mice: mechanisms of mitochondriopathy and cell death. J Comp Neurol 500:20–46.

McDonough H, Patterson C. 2003. CHIP: a link between the chaperone and proteasome systems. Cell Stress Chaperones 8:303–308.

Miller VM, Nelson RF, Gouvion CM, Williams A, Rodriguez-Lebron E, Harper SQ, Davidson BL, Rebagliati MR, Paulson HL. 2005. CHIP suppresses polyglutamine aggregation and toxicity in vitro and in vivo. J Neurosci 25:9152–9161.

Minamiyama M, Katsuno M, Adachi H, Waza M, Sang C, Kobayashi Y, Tanaka F, Doyu M, Inukai A, Sobue G. 2004. Sodium butyrate ameliorates phenotypic expression in a transgenic mouse model of spinal and bulbar muscular atrophy. Hum Mol Genet 13:1183–1192.

Miyazaki K, Fujita T, Ozaki T, Kato C, Kurose Y, Sakamoto M, Kato S, Goto T, Itoyama Y, Aoki M, Nakagawara A. 2004. NEDL1, a novel ubiquitin-protein isopeptide ligase for dishevelled-1, targets mutant superoxide dismutase-1. J Biol Chem 279:11327–11335.

Murayama S, Mori H, Ihara Y, Bouldin TW, Suzuki K, Tomonaga M. 1990. Immunocytochemical and ultrastructural studies of lower motor neurons in amyotrophic lateral sclerosis. Ann Neurol 27:137–148.

Niwa J, Ishigaki S, Doyu M, Suzuki T, Tanaka K, Sobue G. 2001. A novel centrosomal ring-finger protein, dorfin, mediates ubiquitin ligase activity. Biochem Biophys Res Commun 281:706–713.

Niwa J, Ishigaki S, Hishikawa N, Yamamoto M, Doyu M, Murata S, Tanaka K, Taniguchi N, Sobue G. 2002. Dorfin ubiquitylates mutant SOD1 and prevents mutant SOD1-mediated neurotoxicity. J Biol Chem 277:36793–36798.

Niwa J, Yamada S, Ishigaki S, Sone J, Takahashi M, Katsuno M, Tanaka F, Doyu M, Sobue G. 2007. Disulfide bond mediates aggregation, toxicity, and ubiquitylation of familial amyotrophic lateral sclerosis-linked mutant SOD1. J Biol Chem 282:28087–28095.

Pramatarova A, Laganiere J, Roussel J, Brisebois K, Rouleau GA. 2001. Neuron-specific expression of mutant superoxide dismutase 1 in transgenic mice does not lead to motor impairment. J Neurosci 21:3369–3374.

Rosen DR, Siddique T, Patterson D, Figlewicz DA, Sapp P, Hentati A, Donaldson D, Goto J, O'Regan JP, Deng HX, et al. 1993. Mutations in Cu/Zn superoxide dismutase gene are associated with familial amyotrophic lateral sclerosis. Nature 362:59–62.

Ross CA, Poirier MA. 2004. Protein aggregation and neurodegenerative disease. Nat Med 10(Suppl):S10–S17.

Rowland LP, Shneider NA. 2001. Amyotrophic lateral sclerosis. N Engl J Med 344:1688–1700.

Sherman MY, Goldberg AL. 2001. Cellular defenses against unfolded proteins: a cell biologist thinks about neurodegenerative diseases. Neuron 29:15–32.

Shibata N, Asayama K, Hirano A, Kobayashi M. 1996. Immunohistochemical study on superoxide dismutases in spinal cords from autopsied patients with amyotrophic lateral sclerosis. Dev Neurosci 18:492–498.

Shin Y, Klucken J, Patterson C, Hyman BT, McLean PJ. 2005. The co-chaperone carboxyl terminus of Hsp70-interacting protein (CHIP) mediates alpha-synuclein degradation decisions between proteasomal and lysosomal pathways. J Biol Chem 280:23727–23734.

Stam NC, Nithianantharajah J, Howard ML, Atkin JD, Cheema SS, Hannan AJ. 2008. Sex-specific behavioural effects of environmental